



## Biomechanics of a Bifurcating Green Plant, Part 2: Environmental Thermal Effects

W. I. A. Okuyade<sup>1\*</sup> and T. M. Abbey<sup>2</sup>

<sup>1</sup>Department of Mathematics and Statistics, University of Port Harcourt, Port Harcourt, Nigeria.

<sup>2</sup>Applied Mathematics and Theoretical Physics Group, Department of Physics, University of Port Harcourt, Port Harcourt, Nigeria.

### Authors' contributions

This work was carried out in collaboration between both authors. Both authors read and approved the final manuscript.

### Article Information

DOI: 10.9734/AJOPACS/2017/32621

#### Editor(s):

(1) Thomas F. George, Chancellor / Professor of Chemistry and Physics, University of Missouri- St. Louis One University Boulevard St. Louis, USA.

#### Reviewers:

(1) Promise Mebine, Niger Delta University, Nigeria.  
(2) Saima Fazal, South China University of Technology, China.  
(3) Zeeshan Khan, Sarhad University of Science & Information Technology, Pakistan.  
Complete Peer review History: <http://www.sciencedomain.org/review-history/19860>

Original Research Article

Received 5<sup>th</sup> March 2017

Accepted 6<sup>th</sup> April 2017

Published 4<sup>th</sup> July 2017

### ABSTRACT

The effects of environmental temperature differentials on the flow of soil mineral salt water in a bifurcating green plant is presented. The problem involves a set of non-linear differential equations tackled by means of a regular perturbation method. Expressions for the velocity, temperature and concentration, Nusselt number and Sherwood number are obtained, and analyzed graphically. The results indicate that the heat exchange parameter increases the temperature and Nusselt number, while the free convective forces increase the transport velocity and concentration. The increase in these flow variables has tremendous agricultural implications on the growth and productivity of plants (crops). In fact, their increase enhances the rate at which soil water and nutrients are made available to the plants, and this subsequently tends to improve the plant growth and productivity.

*Keywords: Biomechanics; bifurcation; green plants; thermal effects; xylem flow.*

\*Corresponding author: E-mail: [wiaokuyade@gmail.com](mailto:wiaokuyade@gmail.com), [wilsonia6011@gmail.com](mailto:wilsonia6011@gmail.com);

## 1. INTRODUCTION

Green plants play very important roles in the life of man, animal and their environments. They are the ultimate source of food for man and animals. By estimation, they comprise 99% of the biomass.

Amongst others, the xylem and phloem vessels play very important roles in the transport of sap and nutrients in green plants. While the xylem vessels bear the soil mineral salt water from the ground, the phloem vessels bear the sugar manufactured in the leaves through photosynthetic activities. A number of literatures exist on the flow in the vascular bundles of the green plant. Detailed description is found in [1-11]. More so, comprehensive reviews on the flows are given in [12-18]. Similarly, there are some mathematical models on the xylem and phloem flows in green plants. Considering the stem as cylindrical tube with perforations/pores which approximate valves, [19] studied the flow using the method of conformal mapping; [20] and [21] considered the axisymmetrical case of a single pore. [22] examined analytically the xylem and phloem flows at low Reynolds number in a tree trunk with aspect ratio far less than one using the method of Laplace transforms, and observed that, for the phloem flow the concentration is confined near the wall of the green plant and is negative; for the xylem flow the concentration is more valid at the centre, and is positive; the fluids concentration decreases as porosity increases. [23] investigated the effect of diffusion on nutrient transport in a typical green plant, and found that diffusion can be significant at the vessel termini especially if there is an axial efflux of nutrients, and at night when transportation is minimal. [24] studied the biomechanics of a bifurcating green plant by the method of regular perturbation, and noticed that increase in the bifurcation angle increases the velocity, concentration, temperature, Nusselt and Sherwood numbers; the magnetic field decreases the velocity, temperature, and Nusselt number but increases the concentration.

Furthermore, a good number of research reports exist on the fluid dynamics in bifurcating channels. Bifurcation (implying that a flow system divides into two or more daughter channels) phenomenon is seen in both natural and artificial settings. [25] introduced the use of mathematical tools in the study of branching flows; [26] investigated the equilibrium configuration and stability of a channel bifurcation in braided rivers, and showed that an increase in bifurcation angle

increases the transport velocity. [27] investigated a three-dimensional one-to-two symmetrical flow using the method of direct numerical simulation and slender modeling for a variety of Reynolds number and divergent angles, and observed that a flow separation or reversal occurs at the corners of the junction; the inlet pressure increases as the bifurcation angle increases. [28] showed that changes in bifurcation angle alter the flow condition and changes the magnitude of the wall shear stress. [29] studied the flow phenomenon in micro/mini channel networks of symmetrical bifurcation using computer simulation with analytic validation, and found that oscillation amplitude has dominant effects on the streaming velocity in channel networks; the streaming velocity is proportional to the oscillation frequency. Moreover, [30] and [31,32,33] investigated the flow in bifurcating systems, using the method of perturbation series expansions, and noticed that increase in the bifurcation angle, Reynolds number and thermal differentials increase the transport velocity, concentration and Nusselt number of the flow; the Hartmann number decreases velocity.

[22] examined the dynamics of the fluid in the xylem and phloem vessels of the tree trunk whose length is far greater than the diameter (i.e.  $l \gg d$ ) such that the ratio of the length to diameter otherwise called the aspect ratio is far less than one (i.e.  $\mathfrak{R} = d/l \ll 1$ ). According to him, flow in this type of channel is seen to be Poiseuille, laminar and steady. More so, his model found application in green plants like iroko, coconut, paw-paw, plantain and the likes. However, [22] model has some limitations. It considered neither the situation where the plant bifurcates nor the effects of the nature of the soil on the growth and yield of the plant (crop). Therefore, we are motivated to examine, amidst others, the effects of these parameters on the xylem flow. In part one of this study (i.e. in [24]), we considered the effects of bifurcation angles and the nature of the soil on the flow in the trunk of a typical tree plant whose length of trunk is comparable to the diameter of the trunk, and in which case, the ratio of the diameter to the length of the tree trunk is equal to or greater than one. In the said model, [24], the effects of environmental temperature differentials were played down. Therefore, the aim of this paper is to investigate the effects of environmental thermal differentials on the transport of soil mineral salt water through the stem via the branches to the leaves where transpiration and photosynthesis occur with the attendant

implications on the growth and yields of plants (crops).

This paper presents an analytical model on the effect of environmental thermal differentials on the flow of soil mineral salt water in a bifurcating green plant.

The paper is organized in the following manner: section 2 is the material and methods; section 3 gives the results and discussions, and sections 4 holds the conclusions.

## 2. MATERIALS AND METHODS

In a thermal field, there is always a temperature difference, herein called the heat exchange parameter, between the equilibrium temperature of any system and that of its environment. In particular, the environmental temperature depends tremendously on the radiation from the sun, which influences the climatic condition of the region where it is found. At higher environmental temperature, heat is absorbed into the system. The converse may occur when heat is generated in the system or when the environmental temperature drops. In this regard, [22] shows that the thermal gradient can be prescribed as:

$$\frac{\partial T}{\partial r} = h(T_w - T_\infty)$$

where,  $h$  is the film heat transfer coefficient which could be negative. This approximates the Newton's law of cooling. Similarly, every system has its normal or standard temperature

differential level at which it functions best, implying that for a temperature below or above normal, the system becomes inactive or over-active, and is sometimes, destroyed. We shall consider the case where the environmental temperature differential is positive but not above normal.

The problem considers the flow of a fluid of known density in a bifurcating plant when the angles of bifurcation ( $\alpha$  and  $\beta$ ) about the central axis are symmetrical. The xylem vessel is cylindrical and made up of interconnected pores; the mineral salt water is electrolytic, and therefore magnetically susceptible; the fluid viscosity is a function of temperature; the flow has a Reynolds number of about 0.1, and is therefore creeping. If  $\rho$  is the density of the fluid absorbed by the plant;  $p'$  the suction pressure;  $B_o^2$  the magnetic field strength due to saline nature of the soil;  $T'$  is the fluid temperature;  $C'$  is the fluid concentration;  $T_w$  is the temperature at the wall;  $C_w$  is the concentration at the wall of the channel;  $T_\infty$  is the equilibrium temperature of the fluid;  $C_\infty$  is the fluid concentration at equilibrium;  $(u', v', w')$  are the velocity component in the mutually orthogonal  $(r', \theta', x')$  directions in the cylindrical polar coordinates such that assuming the velocity is symmetric

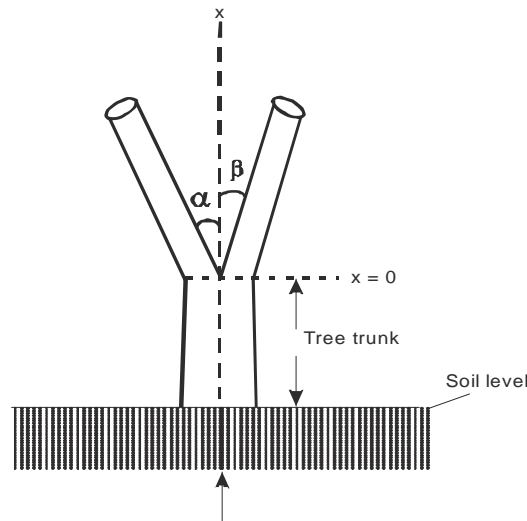


Fig. 1. The physical model of a bifurcating green plant (with symmetric bifurcating angles  $\alpha = \beta$ )

about the  $\theta'$ -axis the problem reduces to two-dimensional with velocity component  $(u', w')$  in the orthogonal  $(r', x')$  direction, then the equations describing the steady flow of soil mineral salt water in a bifurcating green plant in the non-dimensionalized form, considering the Boussinesq approximations are given as follows:

$$\frac{1}{r} \frac{\partial(ru)}{\partial r} + \frac{\Re \partial w}{\partial x} = 0 \quad (1)$$

$$\frac{\partial^2 u}{\partial r^2} + \frac{1}{r} \frac{\partial u}{\partial r} - \frac{u}{r^2} = \frac{\partial p}{\partial r} \quad (2)$$

$$\frac{\partial^2 w}{\partial r^2} + \frac{1}{r} \frac{\partial w}{\partial r} - \left( M^2 + \chi^2 + \frac{\partial w}{\partial x} \right) w = \frac{\Re \partial p}{\partial x} - Gr\Theta - Gc\Phi \quad (3)$$

$$\frac{\partial^2 \Theta}{\partial r^2} + \frac{1}{r} \frac{\partial \Theta}{\partial r} + N^2 \Theta = Pe_h \left( u \frac{\partial \Theta}{\partial r} + \Re w \frac{\partial \Theta}{\partial x} \right) \quad (4)$$

$$\frac{\partial^2 \Phi}{\partial r^2} + \frac{1}{r} \frac{\partial \Phi}{\partial r} + \delta_1^2 \Phi = Pe_m \left( u \frac{\partial \Phi}{\partial r} + \Re w \frac{\partial \Phi}{\partial x} \right) \quad (5)$$

where

$$r = \frac{r'}{R_o}, \quad x = \frac{\Re x'}{l}, \quad w = \frac{R_o w'}{v}, \quad \Theta = \frac{T' - T_\infty}{T_w - T_\infty},$$

$$\Phi = \frac{C' - C_\infty}{C_w - C_\infty},$$

$$p = \frac{(p' - p_\infty) R_o^3}{\rho l v}, \quad Re = \frac{Ul}{v}, \quad M^2 = \frac{\sigma_e B_o^2}{\rho \mu \mu_m},$$

$$N^2 = \frac{Q}{k_o}, \quad \chi^2 = \frac{R_o}{\kappa}, \quad \delta_1^2 = \frac{k_r^2}{D},$$

$$Sc = \frac{v}{D}, \quad Pr = \frac{\mu C_p}{k_o}, \quad Gr = \frac{g \beta_1 (T_w - T_\infty)}{v U}, \quad Gc = \frac{g \beta_2 (C_w - C_\infty)}{v U}$$

$$Pe_m = Re Sc, \quad Pe_h = Re Pr, \quad M_1^2 = \chi^2 + M^2 + \gamma,$$

and  $(u, w)$  are the non-dimensionalized velocities;  $(r, x)$  are the non-dimensionalized cylindrical polar coordinates;  $l$  is the characteristics length of the channel;  $\mu$  is the

fluid viscosity,  $\mu_m$  is the magnetic permeability;

$p$  is the fluid suction pressure;  $p_\infty$  is the fluid pressure at equilibrium;  $\mathbf{g}$  is the acceleration due to gravitational pull;  $\Theta$  and  $\Phi$  are the non-dimensional temperature and concentration, respectively;  $\beta_1$  and  $\beta_2$  are the volumetric expansion coefficient for temperature and concentration respectively;  $\kappa$  is the permeability parameter of the porous medium;  $\sigma_e$  is the electrical conductivity of the fluid;  $k_o$  is the thermal conductivity;  $C_p$  is the specific heat capacity at constant pressure;  $Q$  is the heat absorption coefficient;  $D$  the diffusion coefficient;  $k_r^2$  is the rate of chemical reaction of the soil mineral salt solution;  $\Re$  is the aspect ratio;  $\nu$  is the kinematic coefficient of viscosity;  $R_o$  is the characteristic radius of the tree trunk,  $M^2$  is the magnetic field parameter describing the chemical nature of the soil;  $Re$  is the Reynolds number,  $N^2$  is the environmental temperature differential parameter;  $\chi^2$  is the porosity parameter;  $\delta_1^2$  is the chemical reaction parameter;  $Sc$  is the Schmidt number;  $Pr$  is the Prandtl number;  $Gr$  and  $Gc$  are the Grashof numbers due to temperature and concentration differences, respectively;  $Pe_h$  and  $Pe_m$  are the Peclet numbers due to heat and mass transfers, respectively.

The geometry of the problem as indicated in Fig. 1 shows that the boundary conditions can be split into two distinct parts: the upstream/mother channel,  $x < 0$  and the downstream/daughter channel,  $x > 0$ , and these are given as follows:

for the upstream:

$$(u, w) = (1, 1) \text{ and } (\Theta, \Phi) = (1, 1) \quad \text{at } r = 0 \quad (6)$$

$$(u, w) = (0, 0) \text{ and } (\Theta, \Phi) = (\Theta_w, \Phi_w), \text{ at } r = 1 \quad (7)$$

and

for the downstream:

$$(u, w) = (0, 0) \text{ and } (\Theta, \Phi) = (0, 0) \quad \text{at } r = 0 \quad (8)$$

$$(u, w) = (0,0) \text{ and } (\Theta, \Phi) = (\gamma_1 \Theta_w, \gamma_2 \Phi_w) \text{ at } r = \Re \alpha x \quad (9)$$

(where  $\lambda_1$  and  $\lambda_2$  are constants less than one). The boundary conditions are formulated from [27].

It is readily seen that the equations (1)-(5) are non-linear and highly coupled. We seek for perturbation series solutions of the form:

$$f(r, x) = f_0(r, x) + \xi f_1(r, x) + \xi^2 f_2(r, x) + \dots \quad (10)$$

where  $\xi = \text{Re} < 1$  is the perturbing parameter;  $f_n$  represents the flow variables. Furthermore, we assume the flow is fully developed such that  $\frac{\partial u}{\partial r} = \frac{\partial p}{\partial r} = 0$  ;  $f_0(r, x) = f_{00}(r) - \gamma$  and  $f_1(r, x) = f_{10}(r) - \gamma$  (where  $\gamma$  is a constant) for the upstream and downstream sections, respectively, and specifically  $p = \Re x - \frac{\Re x^2}{\Re}$  for the pressure (where  $\Re x$  is the pressure in the mother region,  $\frac{\Re x^2}{\Re}$  is the pressure in the daughter region) (see [22]), By these, the governing equations (1)-(9) become:

$$\frac{\partial^2 w_{00}}{\partial r^2} + \frac{1}{r} \frac{\partial w_{00}}{\partial r} - M_1^2 w_{00} = \frac{\Re \partial p_{00}}{\partial x} - Gr \Theta_{00} - Gc \Phi_{00} \quad (11)$$

$$\frac{\partial^2 \Theta_{00}}{\partial r^2} + \frac{1}{r} \frac{\partial \Theta_{00}}{\partial r} + N^2 \Theta_{00} = -\gamma \Re Pe_h w_{00} \quad (12)$$

$$\frac{\partial^2 \Phi_{00}}{\partial r^2} + \frac{1}{r} \frac{\partial \Phi_{00}}{\partial r} + N^2 \Phi_{00} = -\gamma \Re Pe_m w_{00} \quad (13)$$

with the boundary conditions

$$w_{00} = 1, \Theta_{00} = 1, \Phi_{00} = 1 \text{ at } r = 0 \quad (14)$$

$$w_{00} = 0, \Theta_{00} = \Theta_w, \Phi_{00} = \Phi_w \text{ at } r = 1 \quad (15)$$

for the upstream, and

$$\frac{\partial^2 w_{10}}{\partial r^2} + \frac{1}{r} \frac{\partial w_{10}}{\partial r} - M_1^2 w_{10} = \Re \frac{\partial p_{10}}{\partial x} - Gr \Theta_{10} - Gc \Phi_{10} \quad (16)$$

$$\frac{\partial^2 \Theta_{10}}{\partial r^2} + \frac{1}{r} \frac{\partial \Theta_{10}}{\partial r} + N^2 \Theta_{10} = -\gamma \Re Pe_h (w_{00} + w_{10}) \quad (17)$$

$$\frac{\partial^2 \Phi_{00}}{\partial r^2} + \frac{1}{r} \frac{\partial \Phi_{00}}{\partial r} + N^2 \Phi_{00} = -\gamma \Re Pe_m (w_{00} + w_{10}) \quad (18)$$

with the boundary conditions

$$w_{10} = 0, \Theta_{10} = 0, \Phi_{10} = 0 \text{ at } r = 0 \quad (19)$$

$$w_{10} = 0, \Theta_{10} = \gamma_1 \Theta_w, \Phi_{10} = \gamma_2 \Phi_w, \gamma_1 < 1, \gamma_2 < 1 \text{ at } r = \Re \alpha x \quad (20)$$

for the downstream.

The upward transport of fluid in green plants through the xylem vessels is enhanced by (a) the suction pressure, which resulted from the osmotic pressure, and (b) the environmental thermal gradient, which culminated in the convective motion of the fluid. For some green plants such as grasses, shrubs and the likes, only the suction pressure is enough to carry the fluid to their terminals, whereas in others such as tall trees, suction pressure and buoyancy factor (Gr/Gc) are required to overcome the gravitational force for the fluid to get to its termini. Therefore, for the case in which the suction pressure is sufficient to transport the fluid from the base to its height, buoyancy is usually neglected such that Gr/Gc=0 (see [22]), and for the other situation where buoyancy is not neglected Gr/Gc≠0. However, this study shall be focused on the situation where Gr/Gc≠0.

An examination of equations (17) and (18) shows that they are still highly coupled, despite the linearization effort. Attempting at solving them, we shall make some assumptions that may lead to solutions that may give approximate pictures of the flow behaviours. We shall eliminate  $w_1$  from equations (17) and (18) by taking  $(D_r - M^2)$  of both sides of them,

where

$$D_r = \left( \frac{\partial^2}{\partial r^2} + \frac{1}{r} \frac{\partial}{\partial r} \right)$$

set  $N^2 = \delta_1^2$ ;  $Pr Gr = ScGc = \varepsilon$  (see [22]) such that  $\Theta_i = \Phi_i$ ; substitute the solutions of  $\Theta_{oo}$  and  $\Phi_{oo}$  into them, and adding the resulting equations, we have

$$\begin{aligned} & \left[ D_r^2 + (N^2 - M_1^2)D_r - (N M_1^2 + 2\gamma\mathfrak{R}\varepsilon) \right] (\Theta_1 + \Phi_1) = -\gamma\mathfrak{R}^2 (Pe_h + Pe_m)(\mathfrak{N} + \mathfrak{N}_1 x) \\ & + 2\gamma\mathfrak{R}\varepsilon \left( L_* I_o(\sigma_+^{1/2} r) - \frac{K_v}{\sigma_+} J_o(\sigma_-^{1/2} r) + N_* I_o(\beta_+^{1/2} r) - \frac{K_w}{\beta_+} J_o(\beta_-^{1/2} r) \right) \end{aligned} \quad (21)$$

Equation (21) is of quadratic form, therefore, we seek for quadratic solutions using

$$\Omega_{\pm} = \frac{-(N^2 - M_1^2) \pm \sqrt{(N^2 - M_1^2)^2 + 4(N^2 M_1^2 + 2\gamma\mathfrak{R}\varepsilon)}}{2}$$

such that it becomes

$$\begin{aligned} & \left[ (D_r - \Omega_-)(D_r - \Omega_+) \right] (\Theta_1 + \Phi_1) = -\gamma\mathfrak{R}^2 (Pe_h + Pe_m)(\mathfrak{N} + \mathfrak{N}_1 x) \\ & + 2\gamma\mathfrak{R}\varepsilon \left( L_* I_o(\sigma_+^{1/2} r) - \frac{K_v}{\sigma_+} J_o(\sigma_-^{1/2} r) + N_* I_o(\beta_+^{1/2} r) - \frac{K_w}{\beta_+} J_o(\beta_-^{1/2} r) \right) \end{aligned} \quad (22)$$

The solutions of equations (11)-(16) and (22) are:

$$\begin{aligned} w_{00}(r) = P_* I_o(M_1 r) - \frac{1}{M_1^2} & \left[ \mathfrak{R}K - Gr \left( L_* I_o(\sigma_+^{1/2} r) - \frac{K_v(r)}{\sigma_+} J_o(\sigma_-^{1/2} r) \right) \right. \\ & \left. - Gc \left( N_* I_o(\beta_+^{1/2} r) - \frac{K_w(r)}{\beta_+} J_o(\beta_-^{1/2} r) \right) \right] \end{aligned} \quad (23)$$

$$\begin{aligned} w_{10}(r) = T_* I_o(M_1 r) - \frac{1}{M_1^2} & \left[ \mathfrak{R}K_1 x - Gr Q_* I_o(\sigma_+^{1/2} r) - \frac{K_y(r)}{\sigma_+} J_o(\sigma_-^{1/2} r) \right. \\ & \left. - Gc \left( S_* I_o(\beta_+^{1/2} r) - \frac{K_y(r)}{\beta_+} J_o(\beta_-^{1/2} r) \right) \right] \end{aligned} \quad (24)$$

for the transport velocity distribution

$$\Theta_{00}(r) = L_* I_o(\sigma_+^{1/2} r) - \frac{K_v(r)}{\sigma_+} J_o(\sigma_-^{1/2} r) \quad (25)$$

$$\Theta_{10}(r) = Q_* I_o(\sigma_+^{1/2} r) - \frac{K_y(r)}{\sigma_+} J_o(\sigma_-^{1/2} r) \quad (26)$$

for the thermal distribution

$$\Phi_{00}(r) = N_* I_o(\beta_+^{1/2} r) - \frac{K_w(r)}{\sigma_+} J_o(\beta_-^{1/2} r) \tag{27}$$

$$\Phi_{10}(r) = S_* I_o(\beta_+^{1/2} r) - \frac{K_y(r)}{\beta_+} J_o(\beta_-^{1/2} r) \tag{28}$$

for the concentration (volume of fluid) distribution

And, the flow Nusselt and Sherwood numbers are:

$$Nu = - \left[ \sigma_+^{1/2} L_* I_1(\sigma_+^{1/2}) + \frac{\sigma_-^{1/2}}{\sigma_+} K_v(1) J_1(\sigma_-^{1/2}) - \frac{K_v'(1)}{\sigma_+} J_o(\sigma_-^{1/2}) \right] \\ - \left[ \sigma_+^{1/2} Q_* I_1(\sigma_+^{1/2} \Re \alpha x) + \frac{\sigma_-^{1/2}}{\sigma_+} K_y(\Re \alpha x) J_1(\sigma_-^{1/2} \Re \alpha x) \right. \\ \left. - \frac{K_y'(\Re \alpha x)}{\sigma_+} J_o(\sigma_-^{1/2} \Re \alpha x) \right] \tag{29}$$

$$Sh = - \left[ \beta_+^{1/2} N_* I_1(\beta_+^{1/2}) + \frac{\beta_-^{1/2} K_w(1) J_1(\beta_-^{1/2})}{\beta_+} - \frac{K_w'(1) J_o(\beta_-^{1/2})}{\beta_+} \right] \\ - \left[ \beta_+^{1/2} S_* I_1(\beta_+^{1/2} \Re \alpha x) + \frac{\beta_-^{1/2}}{\beta_+} K_y(\Re \alpha x) J_1(\beta_-^{1/2} \Re \alpha x) \right. \\ \left. - \frac{K_y'(\Re \alpha x)}{\beta_+} J_o(\beta_-^{1/2} \Re \alpha x) \right] \tag{30}$$

where,  $K$  is the constant suction pressure gradient and  $J_n(z)$  and  $I_n(z)$  are the Bessel and modified Bessel functions of order  $n$  with the argument  $z$ , respectively.

### 3. RESULTS AND DISCUSSION

The effects of environmental thermal differentials on the flow of soil mineral salt water in a bifurcating green plant are considered. To this end, Fig. 2–Fig. 8 show the computational results for the Nusselt number, velocity, temperature and concentration when the heat exchange parameter and Grashof number are varied. For physically realistic constant values of  $Pr = 0.71$ ,  $Re = 0.03$ ,  $\gamma_1 = 0.6$ ,  $\gamma_2 = 0.6$ ,  $\gamma = 0.7$ ,  $\Phi_w = 2.0$ ,  $\Theta_w = 2.0$ ,  $\Re = 0.8$ ,  $\delta_1^2 = 0.2$ ,  $\chi^2 = 0.2$ ,  $M^2 = 0.2$ ,  $\alpha = 5$  and for varying values of  $N^2 = 0.01, 0.1, 0.5, 1.0$ ,  $Gr = 0.1, 0.5, 1.0, 5.0$  the profiles show that the heat exchange parameter  $N^2$  increases the Nusselt number and temperature (see Fig. 2-

Fig. 4); Grashof number increases the velocity and concentration (see Fig. 5-Fig. 8).

The increase in the environmental temperature leads to the absorption of heat from the external source into the plant. The rise in the heat level energizes the fluid particles such that their kinetic energy increases. This increase implies that the particles velocities are increased. And, this tends to account for what is seen in Fig. 2. More so, the increase in the velocity leads to a further increase in the energy level of the plant system. To maintain equilibrium, the excess heat produced is transferred to the wall, for a possible escape by diffusion. The rate at which the heat is transferred is positively influenced by the heat exchange parameter  $N^2$  (see Fig. 3 and Fig. 4).

Furthermore, the increase in the thermal gradient in the presence of gravity generates convective currents, otherwise called the Grashof number, which causes the fluid particles to gain more

energy and reduces the viscous force to make them buoyant. The reduction in the viscous force leads to an increase in the velocity, as seen in Fig. 5 - Fig. 7. This agrees with [30,32] and [33]. It is worthy to notice that the increase in the thermal gradient, which tends to reduce the

viscous force, causes the Reynolds number to rise. Similarly, the increase in the Grashof number leads to increase in the flow velocity, which subsequently increases the rate at which water is made available for transpiration, and quantity of fluid transported.

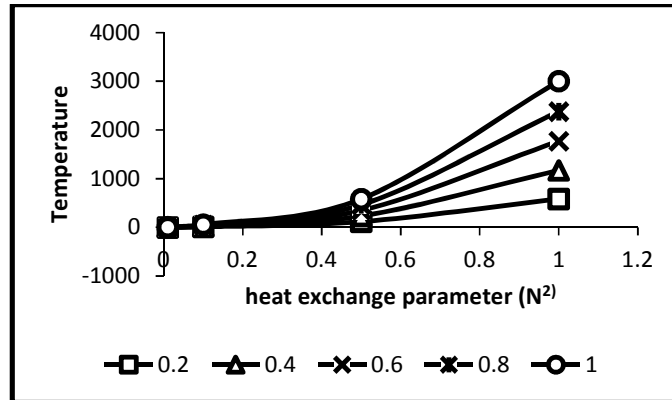


Fig. 2. Temperature profiles for various heat exchange parameter ( $N^2$ ) in the daughter tube

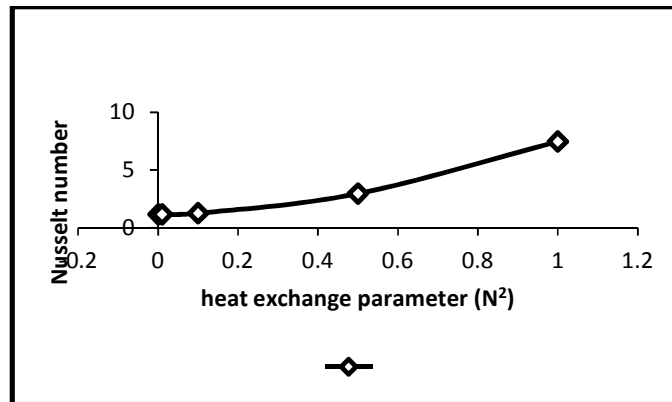


Fig. 3. Nusselt number profiles for various heat exchange parameter ( $N^2$ ) in the mother tube

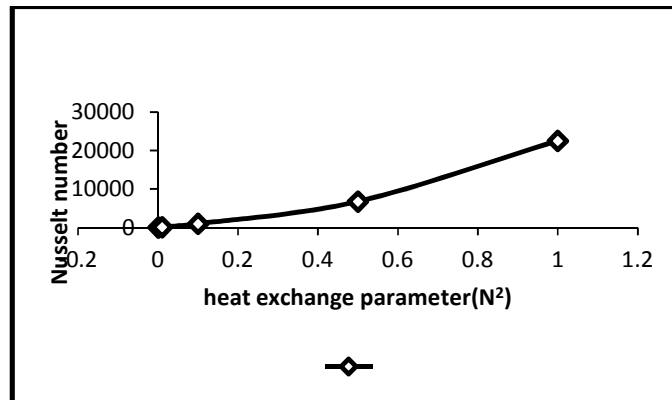


Fig. 4. Nusselt number profiles for various heat exchange parameter ( $N^2$ ) in the daughter tube



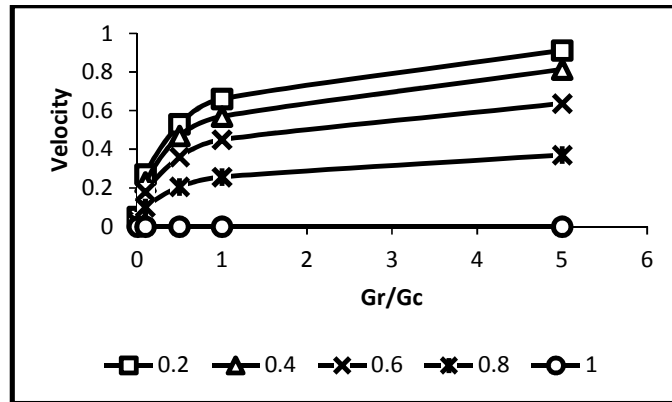


Fig. 5. Velocity profiles for various Grashof numbers (Gr/Gc) in the mother tube

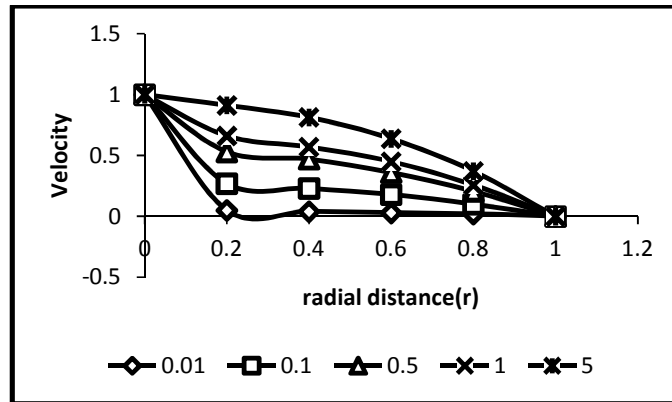


Fig. 6. Velocity-Grashof numbers (Gr/Gc) profiles at various radial distances (r) in the mother tube

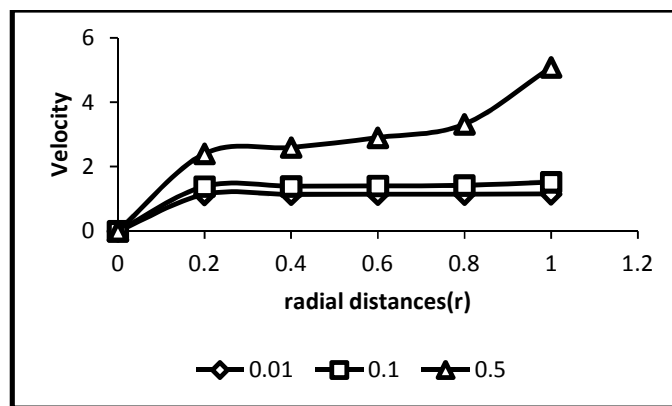
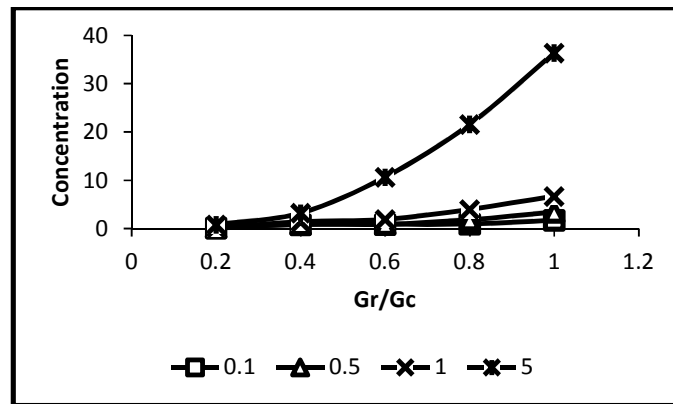


Fig. 7. Velocity-Grashof number (Gr/Gc) profiles at various radial distances (r) in the daughter tube

The increase in the velocity, temperature and concentration has some attendant agricultural implications on the growth potential and productivity of plants (crops). For example, the increase in the environmental temperature leads to soil water evaporation and reduction. At this

stage the water level becomes unreachable to the shallow-rooted plants such that they wither and die. More so, keeping the soil water level constant, the increase in the environmental temperature makes the soil water less viscous, and the plant cell walls more permeable.



**Fig. 8. Concentration-Grashof numbers (Gr/Gc) profiles at various radial distances (r) in the daughter tube**

This tends to increase the absorption of water and nutrients into the plant. Similarly, the increase in the velocity increases the rate at which soil water and nutrients are made available to the plant. Furthermore, the increase in the concentration or quantity of the fluid transported leads to an increase in the nutrients available in the plant; the increase in the concentration of the fluid in the plant means that the fluid is at higher osmotic pressure than that in the soil such that the soil water is compelled into the plant. The results of these processes enhance the plant growth and productivity.

Even so, if other factors affecting photosynthesis are kept constant, the increase in the rate of water transported to the leaves enhances it. Subsequently, this helps in the production of starch (food), and oxygen that enriches our environment.

In addition, transpiration, which is affected by a number of factors such as plants factors (leaf area, leaf structure, and root system), atmospheric factor (sunlight, humidity, temperature and wind) and soil factor (availability of soil water, soil temperature and soil pollution) is enhanced by the availability of water in the plant, as the rate of water absorption must be equal to the rate of transpiration for a healthy plant growth and yield.

#### 4. CONCLUSION

The biomechanics of bifurcating green plants under the influence of environmental temperature variation is presented. The analysis of the results shows that the heat exchange parameter increases the temperature and Nusselt number,

while the free convective forces/Grashof numbers increase the flow velocity and concentration (quantity of fluid transported). The increase in these variables has attendant agricultural implications on the growth and yield of plants/crops. In fact, the increase in the flow velocity and concentration enhances the rate at which soil water and nutrients are made available to the plants (crops), and this subsequently tends to improve their growth and productivity.

#### COMPETING INTERESTS

Authors have declared that no competing interests exist.

#### REFERENCES

1. Crafts AS, Crisp CE. Phloem transport in plants. W. H. Freeman & Co., San Francisco, CA; 1971.
2. Canny MJP. Phloem translocation. Cambridge University Press, Cambridge, England; 1973.
3. Kramer PJ, Boyer JS. Water relations of plants and soils. Academic Press, San Diego; 1995.
4. Tyree MT, Zimmermann MH. Xylem structure and the ascent of sap. Springer, New York; 2002.
5. Holbrook NM, Zwieniecki MA. Eds., Vascular transport in plants. Academic Press, Boston, MA, 1<sup>st</sup> ed.; 2005.
6. Raven PR, Evert, Eichhorn S. Biology of plants. W. H. Freeman and Company Publishers, New York, NY, 7<sup>th</sup> ed.; 2005.
7. Evert RF. Esau's plant anatomy. John Wiley & Sons, Inc., New York. 2006;1-601.

8. Nobel PS. Physicochemical and environmental plant physiology. Academic Press, Boston; 2009.
9. Taiz L, Zeiger E. Plant physiology. Sinauer Associates, Inc., Sunderland, MA, 5<sup>th</sup> ed.; 2010.
10. Morris JR, Hartl DL, Knoll AH, Lue RA, Berry A, Biewener A, Farrell B, Holbrook NM, Pierce N, Viel A. Biology: How life works. W. H. Freeman, New York, NY, 1<sup>st</sup> ed.; 2013.
11. Vogel S. Comparative biomechanics: Life's physical world. Princeton University Press, Princeton, NJ, 2<sup>nd</sup> ed.; 2013.
12. Pickard WF. The ascent of sap in plants. Prog. Biophysical. Molecular Biology. 1981;37:181–229.
13. Rand RH. Fluid mechanics of green plants. Annual Review Fluid Mechanics. 1983;15: 29–45.
14. Karl Niklas, Hanus-Christof Spatz, Julian Vincent. Plant biomechanics: An overview and prospectus. American Journal of Botany. 2006;93(10):1369-1378.
15. Hervé Cochard. The basics of plant hydraulics. The Journal of Plant Hydraulics. 2013;1:e-0001.
16. De Schepper VT, De Swaef I, Bauweraerts, Steppe K. Phloem transport: A review of mechanisms and controls. Journal of Experimental Botany. 2013;64: 4839–4850.
17. Stroock AD, Pagay VV, Zwieniecki MA, Holbrook NM. The physicochemical hydrodynamics of vascular plants. Annual Review Fluid Mechanics. 2014;46:615–642.
18. Bruus H, Holbrook NM, Liesche J, Schulz A, Zwieniecki MA, Bohr T. Sap flow and sugar transport in plants. Reviews Ff Modern Physics. 2016;88(3):035007(1-63). DOI: 10.1103/RevModPhys.88.035007
19. Chapman DC, Rand RH, Cook JR. A hydrodynamic model of bonded pits in conifer tracheids. Journal of Theoretical Biology. 1977;67.
20. Rand RH, Cook JR. Fluid dynamics of phloem flow: An axisymmetric model. Trans. ASAE. 1978;21:898.
21. Rand RH, Upadhyaya SK, Cook JR. Fluid dynamics of phloem II: An approximate formula. Trans. ASAE. 1980;23:581.
22. Bestman AR. Global models for the biomechanics of green plants, part 1. International Journal of Energy Research. 1991;19:677–684.
23. Payvandi S, Daly KR, Jones DL, Talboys P, Zygalakis KC, Roose T. A mathematical model of water and nutrients transport in xylem vessels of a wheat plant. Bulletin of Mathematical Biology. 2014;78:566-596.
24. Okuyade WIA, Abbey TM. Biomechanics of bifurcating green plants, part 1. Asian Journal of Physical and Chemical Sciences. 2016;1(2):1-22.
25. Pedley TJ, Schroter RC, Sudlow MF. The prediction of pressure drop and variation of resistance within the human bronchial airways. Respiratory Physiology. 1970;9: 387–405.
26. Pittaluga MB, Repetto R, Tubino M. Channel bifurcation in braided rivers: equilibrium configuration and stability. Water Resources Research. 2003;39(3): 1046 – 1057.
27. Tadjfar M, Smith FT. Direct simulation and modeling of a 3-dimensional bifurcating tube flow. Journal of Fluid Mechanics. 2004;519:1-32.
28. Soulis. Journal of Biomechanics. 2004;39: 742–749.
29. Zhang Z, Fadl A, Liu C, Meyer DLM. Fluid streaming in micro/mini-bifurcating networks. Journal of Fluid Engineering, ASME. 2009;131:084501-8.
30. Okuyade WIA. MHD blood flow in bifurcating porous fine capillaries. African Journal of Science Research. 2015;4(4): 56-59.
31. Okuyade WIA, Abbey TM. Analytic study of blood flow in bifurcating arteries, part 1-effects of bifurcating angle and magnetic field. International Organization of Scientific Research Journal Mathematics; 2015. I.D: G54040 – (In press)
32. Okuyade WIA, Abbey TM. Analytic study of blood flow in bifurcating arteries, part 2-effects of environmental temperature differentials. International Organization of Scientific Research Journal Mechanical Engineering; 2015. I.D: G54083 – (In press)
33. Okuyade WIA, Abbey TM. Steady MHD fluid flow in a bifurcating rectangular porous channel. Advances in Research (Sciencedomain International). 2016; 8(3):1-17. DOI: 10.9734/AIR2016.26399

**APPENDIX**

$$P_* = \frac{1}{M_1^2 I_o(M_1)} \left[ \Re K - Gr(L_* I_o(\sigma_+^{1/2}) - \frac{K_v(1)}{\sigma_+} J_o(\sigma_-^{1/2})) - Gc(N_* I_o(\beta_+^{1/2}) - \frac{K_w(1)}{\beta_+} J_o(\beta_-^{1/2})) \right]$$

$$K_v(r) = \frac{\sigma_-^{1/2} r^2}{2} \left\{ -\gamma \Re^2 P e_h K + \gamma \Re \mathcal{E} \left( 1 + \frac{\Omega_+ r^2}{4} \right) - \frac{\gamma \Re \mathcal{E}}{\Omega_+} K_u(r) \left( 1 - \frac{\Omega_- r^2}{4} \right) \right\} J_o(\sigma_-^{1/2} r)$$

$$K_u(r) = 1 - \frac{\gamma \Re^2 \mathfrak{K}^2}{2} (P e_h + P e_m) \left( r + \frac{\Omega_- r^3}{2} \right)$$

$$K_w(r) = \frac{\beta_-^{1/2} r^2}{2} \left\{ -\gamma \Re^2 P e_m + \gamma \Re \mathcal{E} \left( 1 + \frac{\Omega_+ r^2}{4} \right) - \frac{\gamma \Re \mathcal{E}}{\Omega_+} K_u(r) \left( 1 - \frac{\Omega_- r^2}{4} \right) \right\} J_o(\beta_-^{1/2} r)$$

$$L_* = \frac{1}{I_o(\sigma_+^{1/2})} \left[ 1 + \frac{K_v(1)}{\sigma_+} J_o(\sigma_-^{1/2}) \right]$$

$$\Omega_+ = \frac{-(N^2 - M_1^2) + \sqrt{(N^2 - M_1^2)^2 + 4(N^2 M_1^2 + 2\gamma \Re \mathcal{E})}}{2}$$

$$\Omega_- = \frac{-(N^2 - M_1^2) - \sqrt{(N^2 - M_1^2)^2 + 4(N^2 M_1^2 + 2\gamma \Re \mathcal{E})}}{2}$$

$$\sigma_+ = \frac{-(N^2 - M_1^2) + \sqrt{(N^2 - M_1^2)^2 + 4N^2 M_1^2}}{2}$$

$$\sigma_- = \frac{-(N^2 - M_1^2) - \sqrt{(N^2 - M_1^2)^2 + 4N^2 M_1^2}}{2}$$

$$\beta_+ = \frac{-(\delta_1^2 - M_1^2) + \sqrt{(\delta_1^2 - M_1^2)^2 + 4\delta_1^2 M_1^2}}{2}$$

$$\beta_- = \frac{-(\delta_1^2 - M_1^2) - \sqrt{(\delta_1^2 - M_1^2)^2 + 4\delta_1^2 M_1^2}}{2}$$

$$\varepsilon = \gamma Pe_h Gr = \gamma Pe_m Gc$$

$$L_* = \frac{1}{I_o(\sigma_+^{1/2})} \left[ 1 + \frac{K_v(1)}{\sigma_+} J_o(\sigma_-^{1/2}) \right]$$

$$K_v(1) = \frac{\sigma_-^{1/2}}{2} \left\{ -\gamma \mathfrak{R}^2 Pe_h K + \gamma \mathfrak{R} \varepsilon \left( 1 + \frac{\Omega_+}{4} \right) - \frac{\gamma \mathfrak{R} \varepsilon}{\Omega_+} K_u(1) \left( 1 - \frac{\Omega_-}{4} \right) \right\} J_o(\sigma_-^{1/2})$$

$$N_* = \frac{1}{I_o(\beta_+^{1/2})} \left[ 1 + \frac{K_w(1)}{\beta_+} J_o(\beta_-^{1/2}) \right]$$

$$K_w(1) = \frac{\beta_-^{1/2}}{2} \left\{ -\gamma \mathfrak{R}^2 Pe_h K + \gamma \mathfrak{R} \varepsilon \left( 1 + \frac{\Omega_+}{4} \right) - \frac{\gamma \mathfrak{R} \varepsilon}{\Omega_+} K_u(1) \left( 1 - \frac{\Omega_-}{4} \right) \right\} J_o(\beta_-^{1/2})$$

$$Q_* = \frac{1}{I_o(\sigma_+^{1/2} \mathfrak{R} \alpha x)} \left[ \gamma_1 \Theta_w + \frac{K_y(\mathfrak{R} \alpha x)}{\sigma_+} J_o(\sigma_-^{1/2} \mathfrak{R} \alpha x) \right]$$

$$K_y(r) = \left[ 1 - \left\{ -\gamma \mathfrak{R} \varepsilon Pe_h (K + K_1 x) + \gamma \mathfrak{R} \varepsilon (L_* I_o(\Omega_+^{1/2} r) - \frac{K_x(r)}{\Omega_+} J_o(\Omega_-^{1/2} r) + L_* I_o(\sigma_+^{1/2} r) - \frac{K_v(r)}{\sigma_+} J_o(\sigma_-^{1/2} r) + N_* I_o(\beta_+^{1/2} r) - \frac{K_w(r)}{\beta_+} J_o(\beta_-^{1/2} r)) \right\} \frac{\sigma_-^{1/2} r^2}{2} \right]$$

$$K_y(\mathfrak{R} \alpha x) = \left[ 1 - \left\{ -\gamma \mathfrak{R}^2 Pe_h (K + K_1 x) + \mathfrak{R} \varepsilon \gamma \left( I_o(\Omega_+^{1/2} \mathfrak{R} \alpha x) + \frac{K_x(\mathfrak{R} \alpha x)}{\Omega_+} J_o(\sigma_-^{1/2} \mathfrak{R} \alpha x) + L_* I_o(\sigma_+^{1/2} \mathfrak{R} \alpha x) - \frac{K_v(\mathfrak{R} \alpha x)}{\sigma_+} J_o(\sigma_-^{1/2} \mathfrak{R} \alpha x) + N_* I_o(\beta_+^{1/2} \mathfrak{R} \alpha x) - \frac{K_w(\mathfrak{R} \alpha x)}{\beta_+} J_o(\beta_-^{1/2} \mathfrak{R} \alpha x) \right) \right\} \frac{\sigma_-^{1/2} (\mathfrak{R} \alpha x)^2}{2} \right]$$

$$K_x(\mathfrak{R} \alpha x) = \left[ 1 - \left\{ -\gamma \mathfrak{R}^2 (Pe_h + Pe_m) (K + K_1 x) + 2\gamma \mathfrak{R} \varepsilon (L_* I_o(\sigma_+^{1/2} \mathfrak{R} \alpha x) - \frac{K_v(\mathfrak{R} \alpha x)}{\sigma_+} J_o(\sigma_-^{1/2} \mathfrak{R} \alpha x) + N_* I_o(\beta_+^{1/2} \mathfrak{R} \alpha x) - \frac{K_w(\mathfrak{R} \alpha x)}{\beta_+} J_o(\beta_-^{1/2} \mathfrak{R} \alpha x)) \right\} \frac{\sigma_-^{1/2} (\mathfrak{R} \alpha x)^2}{2} \right]$$

$$K_v(\Re \alpha x) = \frac{\sigma_-^{1/2}(\Re \alpha x)^2}{2} \left\{ -\gamma \Re^2 P e_h K + \gamma \Re \varepsilon \left( 1 + \frac{\Omega_+(\Re \alpha x)^2}{4} \right) - \frac{\gamma \Re \varepsilon K_u(\Re \alpha x) \left( 1 - \frac{\Omega_-(\Re \alpha x)^2}{4} \right)}{\Omega_+} \right\} J_o(\sigma_-^{1/2} \Re \alpha x)$$

$$K_w(\Re \alpha x) = \frac{\beta_-^{1/2}(\Re \alpha x)^2}{2} \left\{ -\gamma \Re^2 P e_h K + \gamma \Re \varepsilon \left( 1 + \frac{\Omega_+(\Re \alpha x)^2}{4} \right) - \frac{\gamma \Re \varepsilon K_u(\Re \alpha x) \left( 1 - \frac{\Omega_-(\Re \alpha x)^2}{4} \right)}{\Omega_+} \right\} J_o(\beta_-^{1/2} \Re \alpha x)$$

$$K_u(\Re \alpha x) = 1 - \frac{\gamma \Re^2 K}{2} (P e_h + P e_m) \left( \Re \alpha x + \frac{\Omega_-(\Re \alpha x)^3}{4} \right)$$

$$S_* = \frac{1}{I_o(\beta_+^{1/2} \Re \alpha x)} \left[ \gamma_2 \Theta_w + \frac{K_y(\Re \alpha x)}{\beta_+} J_o(\beta_-^{1/2} \Re \alpha x) \right]$$

$$T_* = \frac{1}{M_1^2 I_o(M_1 \Re \alpha x)} \left[ \Re K_{1x} - Gr(Q_* I_o(\sigma_+^{1/2} \Re \alpha x) - \frac{K_y(\Re \alpha x)}{\sigma_+} J_o(\sigma_-^{1/2} \Re \alpha x)) - Gc(S_* I_o(\beta_+^{1/2} \Re \alpha x) - \frac{K_y(\Re \alpha x)}{\beta_+} J_o(\beta_-^{1/2} \Re \alpha x)) \right]$$

© 2017 Okuyade and Abbey; This is an Open Access article distributed under the terms of the Creative Commons Attribution License (<http://creativecommons.org/licenses/by/4.0>), which permits unrestricted use, distribution, and reproduction in any medium, provided the original work is properly cited.

Peer-review history:  
 The peer review history for this paper can be accessed here:  
<http://sciencedomain.org/review-history/19860>